Environmental Earth Sciences (2025) 84:187
https://doi.org/10.1007/s12665-025-12207-2

ORIGINAL ARTICLE

Estimating shear strength parameters of a fine-grained alluvial soil using resedimented samples and multivariate regression

Muhammet Oğuz Sünnetci[1] · **Hakan Ersoy**[1]

Received: 25 July 2024 / Accepted: 16 March 2025
© The Author(s) 2025

Abstract

The number of studies concerning the shear strength of resedimented alluvial soils is extremely limited compared to the studies conducted on fine-grained marine sediments, since alluvial soils are generally tested in remolded or reconstituted state especially in the studies investigating their liquefaction potential. In this study, estimation models were developed to predict cohesion (c) and internal friction angle (ϕ) parameters of a fine-grained alluvial soil using resedimented samples. A total of 60 undisturbed soil samples were obtained from Bafra district of Samsun province (Türkiye) by core drilling. A cone penetration test with pore water pressure measurement (CPTu) was also carried out alongside each borehole to determine the over-consolidation ratios of the samples. Physical-index property determinations and triaxial tests were conducted on the undisturbed samples. 20 sample sets were created with known physical, index, and strength characteristics. The samples are classified as CH, CL, MH, and ML according to the Unified Soil Classification System, with liquid and plastic limits ranging from 31.6–75% and 19.3 to 33.6% respectively. The c and ϕ values of the samples varied from 4.1 to 46.1 kPa and 26 to 35º respectively. The samples were then resedimented in the laboratory under conditions reflecting their original in-situ properties, and triaxial tests were repeated. The c and ϕ values of the resedimented samples ranged from 5.3 to 24.5 kPa and 28 to 32º respectively. The results indicate that the c values of the resedimented samples are generally lower than those of the undisturbed samples, whereas upper and lower bounds for ϕ values are similar. Multivariate regression analyses (MVR) were utilized to develop estimation models for predicting c and ϕ using strength and physical properties of 20 soil samples as independent variables. Three estimation models with R^2 values varying between 0.723 and 0.797 were proposed for c and ϕ which are statistically significant for $p \leq 0.05$. Using artificial neural networks (ANN), the estimation models developed by MVR were replicated to validate the models. ANN yielded very similar results to the MVR, where the R^2 values for the correlations between c and ϕ values predicted by both methods varied from 0.852 to 0.955. The results indicate that c and ϕ values of undisturbed samples can be estimated with acceptable accuracy by determining basic physical and index properties of the disturbed samples and shear strength parameters of the resedimented samples. This approach, which enables the reuse of disturbed soil samples, can be used when undisturbed soil samples cannot be obtained from the field due to economic, logistical, or other reasons. Further research on the shear strength parameters of resedimented alluvial soils is needed to validate the estimation models developed in this study and enhance their applicability to a wider range of alluvial soils.

Keywords Artificial neural networks · Fine-grained alluvial soil · Multivariate regression analysis · Resedimentation · Cohesion · Internal friction angle

Introduction

The shear strength of soils is a crucial input parameter in almost all civil engineering applications in the soil environment. Soil shear strength is expressed in terms of two key parameters, cohesion (c) and internal friction angle (ϕ). c refers to the amount of bonding between soil particles, generally related to shear stresses and cementation, while ϕ is the angular representation of the resultant frictional forces

✉ Muhammet Oğuz Sünnetci
moguzsunnetci@ktu.edu.tr

[1] Faculty of Engineering, Department of Geological Engineering, Karadeniz Technical University, 61080 Trabzon, Turkey

Published online: 28 March 2025

within the soil. These parameters are determined either in the field or in the laboratory by various tests. Yet, the majority of in-situ tests are extremely difficult and costly, and sometimes impossible to conduct due to limitations of the test and the test site. Therefore, laboratory tests are generally preferred to determine the shear strength parameters required for engineering design. It is very well known that the accuracy and reliability of laboratory test results are directly related to the quality of the test sample. Especially for sensitive tests such as triaxial compressive strength, high-quality undisturbed soil samples are essential. However, obtaining undisturbed samples from the field requires costly applications such as double-tube core drilling, and the use of special equipment like piston samplers with vacuum locks. Even then, although the obtained sample is considered as undisturbed, varying degrees of disturbance could occur within the sample during transport, storage, and extrusion from the sampler.

To overcome the above limitations and difficulties, researchers tried to estimate the shear strength parameters of undisturbed soils using index and physical properties of the disturbed samples. The studies utilized statistical approaches such as correlation or regression analyses (Sørensen and Okkels 2013; Stark and Hussain 2013; Khaboushan et al. 2018), or, more recently, soft computing and/or machine learning algorithms (Goktepe et al. 2008; Ersoy et al. 2013; Tran et al. 2022; Pham et al. 2021; Rabbani et al. 2023; Mohammadi et al. 2022; Mousavi et al. 2011; Zhu et al. 2022.). Different types of samples were also used in the corresponding studies, from over-consolidated undisturbed samples to disturbed samples. Atterberg limits, clay fraction, grain size distribution, and density are among the most used parameters in the analyses.

Due to their granular and porous structure, soils can easily lose their original properties as a result of external factors. In addition, soils can show different properties over very short distances due to weathering processes, stress, groundwater conditions, etc. For this reason, even soil samples taken from the same environment can show significant heterogeneity. Kul Yahşi and Ersoy (2021), in their study on residual clays up to 10 m thick and widely distributed in Trabzon province (Türkiye), found that clays can exhibit very different geotechnical properties in both horizontal and vertical directions, even at very short distances, and reported that chemical processes and bedrock topography are at work in the large variation of soil properties over depths of several meters. This makes it difficult to systematically investigate the behavior of the soil material under different stress and load conditions. Laboratory-compacted (or artificial) soil samples, on the other hand, can be produced in a controlled environment where parameters such as void ratio, water content, grain size, pre-consolidation stress, and stress history can be arranged as desired. As all produced samples share the same properties, systematical investigation of certain soil parameters can be conducted. In the literature, 3 different types of laboratory-compacted samples have been used by researchers. Remoulded samples are those formed by mixing and compacting natural soil samples at different water contents (Kayabali and Tufenkci 2010; Miao et al. 2006). Reconstituted specimens are those formed by thoroughly mixing natural soil samples in water contents 1–1.5 times their liquid limit and consolidating or compacting them in one dimension (Burland 1990). Resedimented specimens are formed by drying, grinding, and mixing particularly cohesive soil samples in a water content of 2 times their liquid limit and consolidating them under increasing stress (Ladd and Varallyay 1965).

Laboratory-compacted soil samples are being increasingly preferred by researchers for geotechnical testing under varying stress and failure mode conditions to systematically investigate the soil's strength or consolidation characteristics (Ladd and Varallyay 1965; Locat and Lefebvre 1985; Burland 1990; Cunningham et al. 2003; Abdulhadi et al. 2012; Casey et al. 2019; Wang et al. 2023), stiffness and permeability anisotropy (Ranjpour 2020; Marjanovic 2016; Nordquist 2015; Adams et al. 2016; Santagata and Kang 2007; Seah 1990), or deformation characteristics (Huang and Swan 2017; Casey et al. 2015a). On the other hand, studies focusing on estimating shear strength properties of intact samples using laboratory-compacted samples are very scarce. Some researchers (Burland 1990; House 2012; Casey et al. 2015b) compared intact and resedimented behavior of different fine-grained soils, yet no estimation model was suggested in these studies to predict the shear strength parameters of the undisturbed samples.

Considering the above-mentioned gap in the literature, the aim of this study was to estimate the shear strength parameters of undisturbed alluvial soil samples using the plastic and index properties of disturbed samples, as well as the shear strength parameters of resedimented samples. Using custom-made thin-walled UD samplers, 60 undisturbed samples were obtained from a young alluvial soil deposit in the Bafra district of Samsun city (Türkiye) by core drilling in 5 locations. Next to each borehole a cone penetration test was also conducted to determine the over-consolidation ratios of the obtained samples. Index, physical, and shear strength parameters of the acquired undisturbed samples were determined in the laboratory. The samples were then resedimented in the laboratory under consolidation stresses equivalent to their in-situ effective overburden stresses. The shear strength parameters of the resedimented samples were then determined. Finally, multivariate regression analyses were conducted for 20 sample sets, using index, physical, and shear strength parameters of the resedimented samples as independent variables to estimate the strength parameters of undisturbed samples.

Material and methods

Location and geological properties of the study area

Soil samples were collected from Sahilkent village, located 12 km northwest of Bafra district in Samsun province, Türkiye. The area is situated in the Eastern Pontides Orogenic Belt (EPOB), which is an extension of the Alpine-Himalayan mountain building system in Türkiye. The EPOB is an igneous arc that spans approximately 500 km in length and 200 km in width (Eyüboğlu 2011). It extends to the Georgian border in the east and is bounded by the Central Pontides in the west, the Eastern Black Sea Basin in the north, and the Anatolide-Tauride Block in the south (Okay 2008).

The Bafra region is located at the northwestern end of the EPOB, bordering the Central Pontides (Temizel et al. 2016). The Cankurtaran Formation, dating back to the Late Cretaceous period, is the oldest unit in the region (Görür and Tüysüz 2001). It is composed of sandstone and shale interbedded with tuff-tuffite, sandy limestone, and marl. The Akveren Formation, dating back to the Late Cretaceous-Early Palaeocene period, overlies the Cankurtaran Formation and is composed of sandstone, sandy limestone, limestone, and siltstone (Görür and Tüysüz 2001). The Atbaşı Formation, dating back to the Late Palaeocene-Early Eocene period, conformably overlies these units (Gedik et al. 1984). The unit comprises limestone, sandy limestone, sandstone, and marl interbeds. It is unconformably overlain by the Middle Eocene Kusuri Formation, which consists of sandstone-marl-shale interbedded limestones (Gedik and Korkmaz 1984; Aydın et al. 1995; Görür and Tüysüz 2001. The Tekkeköy Formation, which consists of Eocene basalts and andesites, unconformably overlies the Kusuri Formation (Gedik et al. 1984).

The alluvial deposits that are the subject of this study are located in the Sahilkent region (Fig. 1). In this region, the alluvial material of Kızılırmak, the river with the second largest drainage area in Türkiye, is exposed over a very large area (Turoğlu 2010). The alluvial material is divided into two parts as Late Quaternary (Holocene) new alluvium

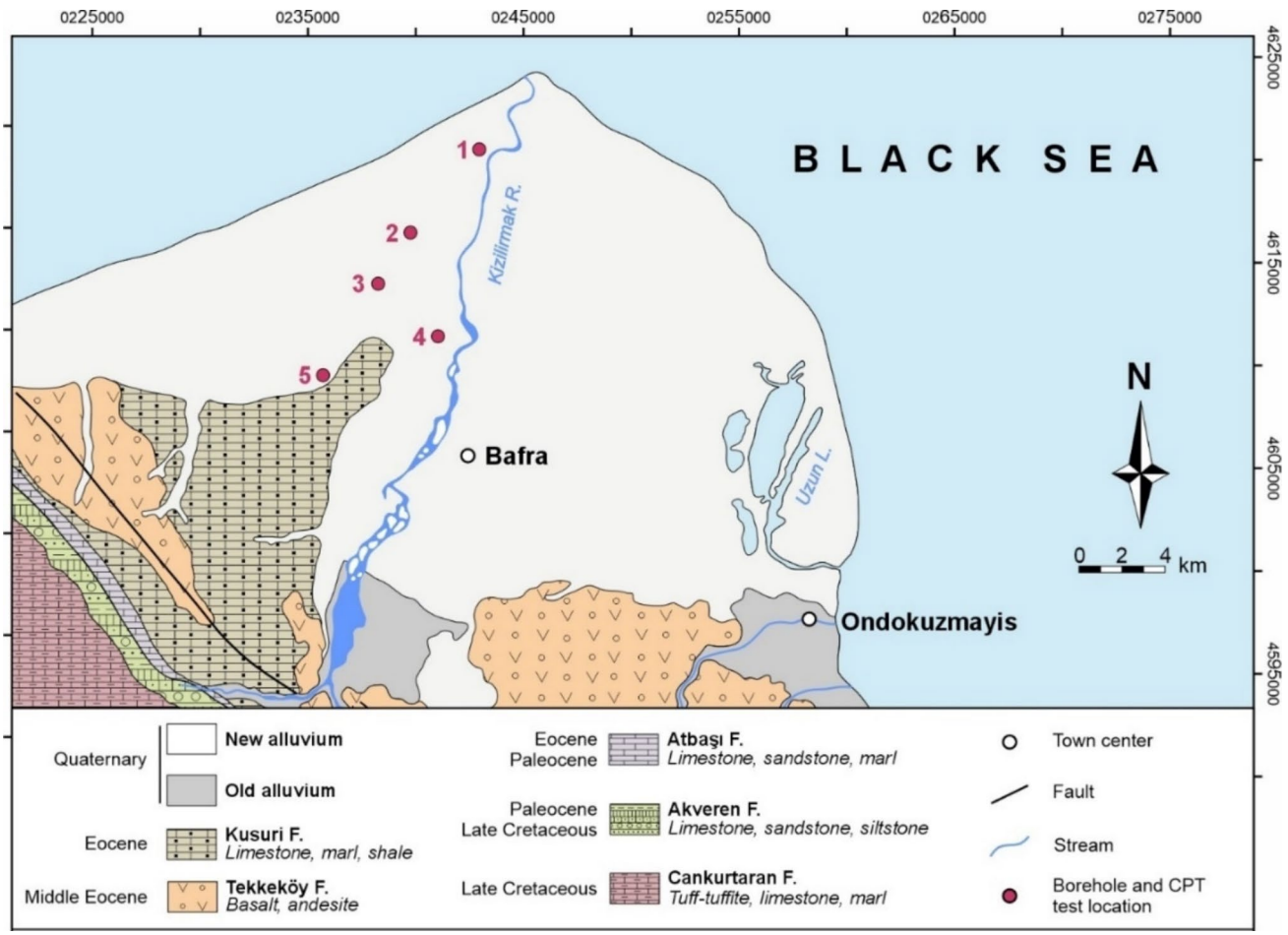


Fig. 1 Geological map of the study area

and Early Quaternary (Pleistocene) old alluvium. While the old alluvium is generally found in the form of fields and tablelands, the new alluvium covers the present riverbed and partly the Black Sea coast. The wetland and plain area where the old and new alluvium are located is called the current delta plain or Bafra coastal plain (Turoğlu 2010; Sünnetci and Ersoy 2021). The soil samples used in this study were collected from the Holocene-aged new alluvium.

Acquisition of undisturbed samples

The study area was drilled with five 10-m-deep boreholes, and undisturbed soil samples were collected using custom-made UD samplers that are 9 cm in diameter and 60 cm in length (maximum sample length is 50 cm) with 2 mm of wall thickness. The samplers were made from a chromium-iron alloy and their uppermost section was perforated to permit the escape of air during penetration. To minimize sample disturbance, a silicon-based lubricant agent was sprayed on the inner wall of the samplers, and the samplers were driven into the soil using hydraulic pressure without rotation. No drilling fluid was used. Groundwater was encountered at a depth of 2–3 m. To ensure maximum saturation, undisturbed samples were collected between 4 and 10 m since laboratory-sedimented samples will be fully saturated. 60 undisturbed samples were collected from all 5 boreholes, with a single undisturbed sample collected every 50 cm. Upon collection, the samples were immediately waxed, wrapped, and labelled with their respective ID and depth (Fig. 2).

As mentioned above, 60 undisturbed soil samples were collected from the boreholes. However, obtaining 3 triaxial test specimens from one UD sampler to determine cohesion and internal friction angle would be practically difficult. Therefore, a single triaxial test specimen was obtained from each sampler. This way, 3 specimens obtained from 3 consecutive UD samplers were considered as a single set of samples. The soil remaining in each UD sampler was used to determine its plastic and index properties. Ultimately, 20 sample sets were created with known index, plastic, and strength properties.



Fig. 2 Acquisition and labeling of the undisturbed soil samples

Cone penetration tests (CPT)

CPT is one of the most preferred in-situ tests in the field of geotechnical engineering which allows evaluation of soil behavior, grain size distribution, over-consolidation ratio (OCR), pore water pressure, and undrained shear strength. The test is based on the principle of penetrating a cone-shaped device into the soil and recording the resistance at the cone tip and the friction at the cone sleeve using electronic sensors. Fine-grained soils generally have low cone tip resistance—high sleeve friction values, while coarse-grained soils have high cone tip resistance—low sleeve friction values (Robertson 1990). In this study, the data from the CPT tests were used to estimate the grain size characteristics of the soil profile and calculate OCR.

As part of this study, 5 CPTu boreholes, each 15 m deep, were drilled using piezocones, which can also measure pore water pressure. The CPTu sounding locations were selected to be very close to the boreholes (horizontal distance < 1 m) to ensure the best representation of undisturbed samples. The sounding speed did not exceed 2 cm/sec and parameters such as sleeve friction, tip resistance, pore water pressure, and effective stress were recorded every 5 cm. These data were averaged for every 50 cm to correlate the results with the undisturbed samples. Normalized tip resistance (Q_{tn}) and normalized sleeve friction (F_r) values were calculated as suggested by Robertson (2009) to negate the effect of increasing effective pressure with depth. When calculating OCR by CPTu data, the below suggested by Kulhawy and Mayne (1990) was used because it can be applied to a very wide range of soils and uses the Q_{tn} parameter which was already calculated for all CPTu soundings during soil classification phase:

$$OCR = kQ_{tn}$$

where k is the pre-consolidation cone factor which changes in a range of 0.2–0.5, typically assumed as 0.33. Considering the grain size distributions of the samples, a k value of 0.2 was used in this study. Soil behavior types of the samples were also determined according to the method suggested by Robertson (1990) using Q_{tn} and F_r.

Laboratory tests

Laboratory tests were conducted to determine the natural water content, natural unit weight, specific gravity, void ratio, saturation degree, Atterberg limits, and grain size distribution of all samples. The tests were carried out in

Table 1 Sample types and test standards used in laboratory testing for various soil parameters

Test parameter	Sample type	Standard
Natural water content	Undisturbed	ASTM D2216
Specific gravity	Disturbed	ASTM D854
Plastic limit	Disturbed	ASTM D 4318
Liquid limit	Disturbed	BS 1377–2:1990
Grain size distribution	Disturbed	ASTM D6913
c, ϕ	Undisturbed	ASTM D2850
c, ϕ	Resedimented	ASTM D2850

accordance with the corresponding international standards (Table 1), or by using phase relation equations among the parameters determined during the tests. The shear strength parameters, cohesion (c) and internal friction angle (ϕ), of the samples were determined through unconsolidated-undrained (UU) triaxial tests using a servo-controlled semi-automatic testing system. Triaxial tests were conducted on standard specimens with a diameter of 3.8 cm and a length of approximately 8 cm. The tests were conducted under confining pressures of 50, 100, and 200 kPa (OCR = 1–5) with a shear rate of 0.5 mm/min until 20% strain was reached. The same testing procedure was performed on resedimented samples to determine their shear strength parameters.

Resedimentation procedure

Prior to resedimentation, the physical and mechanical properties of undisturbed soil samples were determined as outlined in Subsection "Cone Penetration Tests (CPT)". These samples were then subjected to resedimentation using the consolidometers designed in this study (Fig. 3). The design of the consolidometers is based upon a typical triaxial testing cell with some modifications to enable slurry consolidation. This approach was adopted because it is comparatively easier than manufacturing the device from the ground up, thus making resedimentation method more accessible for the researchers around the world. The designed consolidometers have no obvious advantages over the ones used in the literature, but they are quite easy to manufacture and functional enough to allow adequate control over the samples to prepare them as closely as possible to the intact samples. Each resedimented sample was subjected to an increasing consolidation stress during resedimentation, up to a maximum equal to the effective overburden stress at the depth from which the sample was taken from the boreholes.

The disturbed samples were then resedimented in the laboratory using a method similar to the one conducted at MIT (Casey et al. 2015a). The disturbed soil sample was dried in an oven at 105 ℃ for 24 h and ground in a ring grinder to pass through a #100 sieve. Approximately

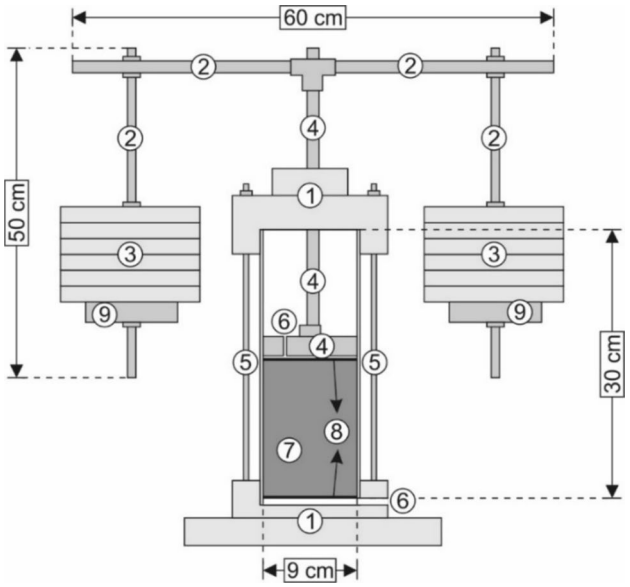


Fig. 3 The schematic of the consolidometer designed and used in this study (1: top and bottom caps; 2: loading arm; 3: weights; 4: piston and piston rod; 5: stabilizing shaft; 6: water discharge outlet; 7: sample; 8: porous stones and filter papers; 9: load stabilizer) (Sünnetci 2022)

1 kg of material was ground for each resedimented sample to be prepared. The soil sample was mixed with de-aired distilled water at twice its initial liquid limit in weight. To achieve a homogeneous mixture, the slurry was initially mixed with a laboratory mixer for 10 min. However, due to the high degree of agglomeration in the samples prepared in this manner, the mixing process was completed manually. The resulting homogeneous slurry was then slowly poured into a consolidometer with filter paper at the bottom to prevent air bubbles. The slurry was allowed to settle for 24 h. After this time, a piston with filter paper at the bottom was placed on top of the sample and the top cover of the consolidometer was tightly closed. The loading arms were then attached to the top cover and an initial load of 0.5 kg (approximately 2.5 kPa of stress) was applied to the sample. The stress was then gradually increased until the desired consolidation stress was achieved. Each loading step was applied for 24 h. The final loading step was applied for 48 h to allow secondary compression of the sample (Abdulhadi 2009). After the resedimentation process was complete, the load on the sample was removed while holding the piston stationary. The sample was then removed from the consolidometer by gently pushing the piston (Fig. 4).

Even though almost identical samples can be produced by resedimentation, some degree of stratification can occur within the samples during the precipitation of the soil material by gravity. Besides, the particles in the soil can be



Fig. 4 Preparation and extrusion of a resedimented soil sample: resedimentation (**a**) and extrusion (**b**, **c**, **d**), and preparation of a resedimented triaxial test sample (**e**, **f**)

re-arranged according to the effective stress applied during the consolidation phase (Delage and Lefebvre 1984).

Multivariate regression analysis

Multivariate regression (MVR) analyses were conducted on the physical and mechanical properties of undisturbed and resedimented samples to predict the cohesion and internal friction angle values of the undisturbed samples. The MVR analyses were performed using IBM SPSS Statistics v23 software. The stepwise method was used in the MVR analyses, where one additional independent variable is included in the model at each step based on their standardized beta values. The standardized beta value indicates the strength of the effect of each independent variable on the dependent variable in a unit-free manner, and its absolute value is considered. In addition, the significance of each independent variable is also tested at 95% confidence interval (CI) and insignificant (Sig. > 0.05) variables were removed. In order to propose reliable estimation models, equations that have coefficient of correlation (R) values lower than 0.8 and/or coefficient of determination (R^2) values lower than 0.7 were discarded. Linear models were preferred to nonlinear ones for ease of application, unless there was a large difference in R and R^2 values.

Results

Index and physical properties of the soil samples

The wet sieve analysis test results show that the samples contain 18–63% clay, 29–67% silt, and 8–28% sand-sized materials (Table 2). The granulation curves of all samples are given in Fig. 5. There is no gravel in the samples. The natural water content of the samples varies between 22 and 39% (Table 3). The values of the degree of saturation (Sr) and the void ratio (e) obtained from the tests on the cylindrical specimens prepared for the UU triaxial test range from 90.4 to 97.5% and from 59.4 to 93.2%, respectively. The pycnometer tests revealed that the samples had a specific gravity ranging from 2.50 to 2.69. The natural unit weight values varied between 17.3 and 19.5 kN/m^3. The liquid limits ranged from 31.6 to 75%, while the plastic limits ranged from 19.3 to 33.6% (Table 4). The plasticity indices varied from 11.8 to 43.6%. Table 4 shows that the majority of soil samples used in the tests belong to the low plasticity clay class, with a few exceptions classified as high plasticity clay, high plasticity silt, and low plasticity silt according to the Unified Soil Classification System (USCS) (ASTM D2487-17).

Table 2 Grain size distributions of the samples

Sample set	Clay (%)	Silt (%)	Sand (%)	Sample set	Clay (%)	Silt (%)	Sand (%)
1	27	57	16	11	50	38	12
2	32	43	25	12	22	67	11
3	31	59	10	13	18	59	23
4	18	54	28	14	34	56	10
5	28	63	9	15	38	50	12
6	30	58	12	16	32	59	9
7	42	47	11	17	33	53	14
8	50	43	7	18	21	56	23
9	63	29	8	19	26	60	14
10	52	39	9	20	29	61	10

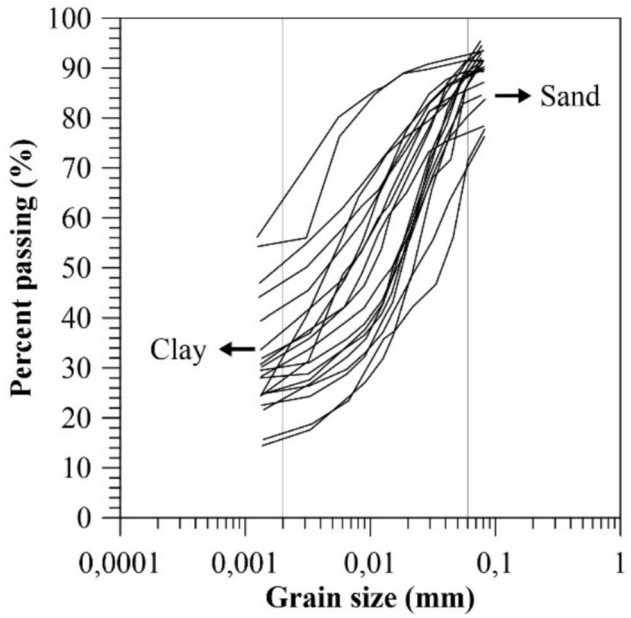


Fig. 5 Granulometry curves of all samples

CPTu test results

Results of the CPTu tests are given in Table 5. As an example, CPTu data obtained from CPTu-1 (which is next to Borehole-1), as well as the normalized soil behavior types of the samples, are given in Fig. 6. The samples are classified as clay and silt-mixtures, which is in accordance with the results of the USCS classification. A generalized profile of the subsurface was derived from CPTu data (Fig. 7). OCR values determined by CPTu data are presented in Table 5. As can be seen, although the alluvial material is relatively young, the samples are moderately over-consolidated, probably because of the lowering of the groundwater table (GWT) over the years.

Mechanical properties of the undisturbed samples

Based on the UU triaxial test data, the samples showed a range of cohesion values between 4.1 and 46.1 kPa, and internal friction angles between 26 and 35 degrees (Table 6). It is important to note that in UU triaxial tests performed on fully saturated soils, the pore water pressure cannot be attenuated, resulting in an expected internal friction angle value of zero and a horizontal Mohr's failure envelope at all confining pressures. However, the samples used in this study

Table 3 Void ratio, natural water content, natural unit weight, and saturation degree values of the samples

Sample set	e (%)	ω_n (%)	γ_n (KN/m^3)	S_r (%)	Sample set	e (%)	ω_n (%)	S_r (%)	γ_n (KN/m^3)
1	88.4	30	18.0	91.4	11	91.5	39	96.0	17.3
2	89.9	33	17.8	95.2	12	77.4	27	93.2	18.7
3	83.3	30	18.6	96.3	13	87.7	30	90.8	18.1
4	59.4	22	19.5	97.5	14	71.1	25	92.6	18.8
5	93.2	33	18.1	93.6	15	80.9	38	96.8	18.5
6	81.8	28	18.1	90.8	16	81.4	34	97.2	18.2
7	79.6	29	17.7	91.4	17	77.7	38	96.9	18.0
8	92.7	33	17.5	91.6	18	78.8	34	95.7	18.4
9	80.8	28	17.7	90.4	19	79.2	29	94.4	18.6
10	86.5	33	17.6	95.2	20	73.2	30	93.5	18.8

Table 4 Atterberg limits and USCS classes of the samples

Sample set	PL (%)	LL (%)	PI (%)	USCS class	Sample set	PL (%)	LL (%)	PI (%)	USCS class
1	21.2	41.4	20.2	CL	11	33.6	57	23.4	CL
2	19.7	31.6	11.9	CL	12	22.1	34.4	12.3	CL
3	19.3	46.1	26.8	CL	13	24.6	37.5	12.9	CL-ML
4	27.4	41.9	14.5	ML	14	21.5	33.5	12.0	CL
5	22.7	40.4	17.7	CL	15	28.8	62.2	33.4	CH
6	23.6	35.4	11.8	CL	16	26.4	53.9	27.5	CH
7	21.6	46	24.4	CL	17	31.8	55.5	23.7	MH
8	29.1	58	28.9	CH-MH	18	25.6	45.4	19.8	CL
9	32.3	73.5	41.2	CH-MH	19	22.9	35.4	12.5	CL
10	31.4	75	43.6	CH	20	21.4	42.9	21.5	CL

Table 5 Results of the CPTu tests conducted in the study area

S.S.	Q_{tn}	F_r	OCR	I_C	S.S.	Q_{tn}	F_r	OCR	I_C
1	20.02	1.71	4.0	2.61	11	25.50	7.30	5.1	2.93
2	15.20	5.97	3.0	3.04	12	11.15	8.00	2.2	3.22
3	21.81	4.42	4.4	2.83	13	30.46	3.62	6.1	2.67
4	16.39	3.99	3.3	2.90	14	15.30	6.31	3.1	3.05
5	45.24	1.81	9.0	2.34	15	20.93	8.51	4.2	3.04
6	24.11	3.65	4.8	2.75	16	11.04	8.39	2.2	3.24
7	26.97	3.98	5.4	2.73	17	24.18	4.56	4.8	2.81
8	12.91	7.98	2.6	3.17	18	15.63	6.35	3.1	3.04
9	32.81	2.89	6.6	2.58	19	21.83	7.95	4.4	3.01
10	21.27	5.29	4.3	2.89	20	12.26	8.17	2.5	3.20

SS Sample set

were not fully saturated, with degree of saturation ranging from 90.4 to 97.5%. Therefore, internal friction angle values higher than zero were obtained.

Normally, the saturation degree of the undisturbed samples gathered from below the GWT should be close to 100%, or at least higher than 95%. Yet, in this study this is not the case because of the matric suction occurring between the soil layers just below and above the GWT, which is at a depth of 2–3 m throughout the study area. Because of the matric suction, even the samples acquired from below the GWT can be unsaturated as they lose some of their water content to the soil above the GWT. Furthermore, the extended procedure for extracting and trimming a sample, measuring its dimensions, weighing it for reference, and then assembling a triaxial test chamber results in a certain degree of moisture loss in the samples.

Nevertheless, it is quite clear that the internal friction angle values determined in this study seem unusually high, especially at such saturation degrees. On the other hand, considering the grain size distributions of the samples, which vary from clay to sandy silt, and their plasticity, which is low for almost all samples, the results can be considered as reasonable. Table 6 summarizes the results of the triaxial tests conducted on undisturbed soil samples.

Mechanical properties of the resedimented samples

The resedimented samples were prepared from the samples tested in the first phase of the study. As the index and plastic parameters, including LL, PL, grain size distribution, and specific gravity, remained unchanged between the samples, no plastic or index property determinations were made on the resedimented samples. Only UU triaxial tests were performed under the same conditions as the tests on the undisturbed samples. The results are summarized in Table 7. It is seen that the c values of the resedimented samples vary from 5.3 kPa to 24.5 kPa, whereas ϕ values vary from 28° to 32°.

As previously stated, the resedimented samples are expected to be fully saturated. Therefore, the internal friction angle values obtained from the UU triaxial tests performed on these samples should be zero. However, Table 6 shows that internal friction angle values ranging from 28 to 31 degrees were obtained, indicating that the resedimented samples were not fully saturated. Saturation degree values of 9 resedimented samples varied between 88 and 97%. It is thought that this is because air fills some of the gaps in the samples due to matric suction resulting from the release of vertical stress after the resedimented samples were taken out

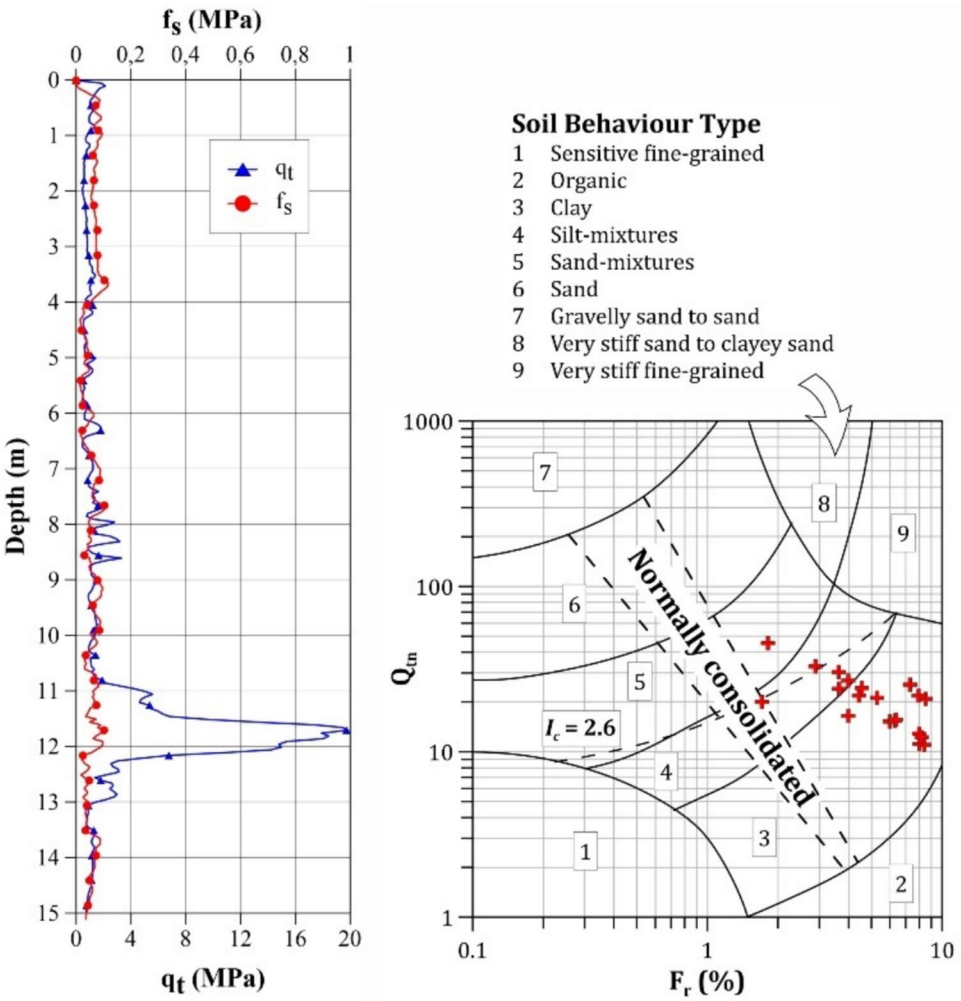


Fig. 6 Cone tip resistance (q_t) and sleeve friction (f_s) values obtained by the CPTu sounding next to Borehole-1 (left) and soil behavior type classification for all CPTu soundings (right)

of the consolidometer. It is also possible that the silt content of the resedimented samples is higher than the intact samples, since they are prepared from materials passing through a #100 sieve.

Prediction of the mechanical properties of undisturbed soil samples

Correlation analyses

Correlation analyses were used to develop a model for estimating the shear strength parameters of undisturbed samples using resedimented samples. At the first stage, relationship between the shear strength parameters of undisturbed and resedimented samples was investigated by creating scatter plots using the c and ϕ values of both types of samples. When evaluating the significance of statistical relationships, we considered the correlation coefficient values. The plots are given in Fig. 8.

As can be seen in Fig. 8, correlation analyses of c and ϕ parameters of resedimented and undisturbed samples indicate no significant relationship between these parameters. This holds true even for samples with similar liquid limit, plastic limit, grain size distribution, unit weight, or specific gravity values, or samples taken from almost the same depth. This indicates that two variables are insufficient for obtaining a significant result in statistical analysis, and more parameters should be included. Therefore, in the second stage, MVR analyses were conducted, including physical and index parameters of soil samples.

MVR analyses

The MVR analyses were conducted by including the physical, index, and shear strength parameters of undisturbed and resedimented samples. Table 8 shows the parameters and types of variables used in the MVR analyses. These parameters were included in the MVR analyses because they are among the most commonly used parameters in characterizing soils in terms of their physical and plastic properties and are determined in almost every application of geotechnical studies. Also, these are the main input parameters used in

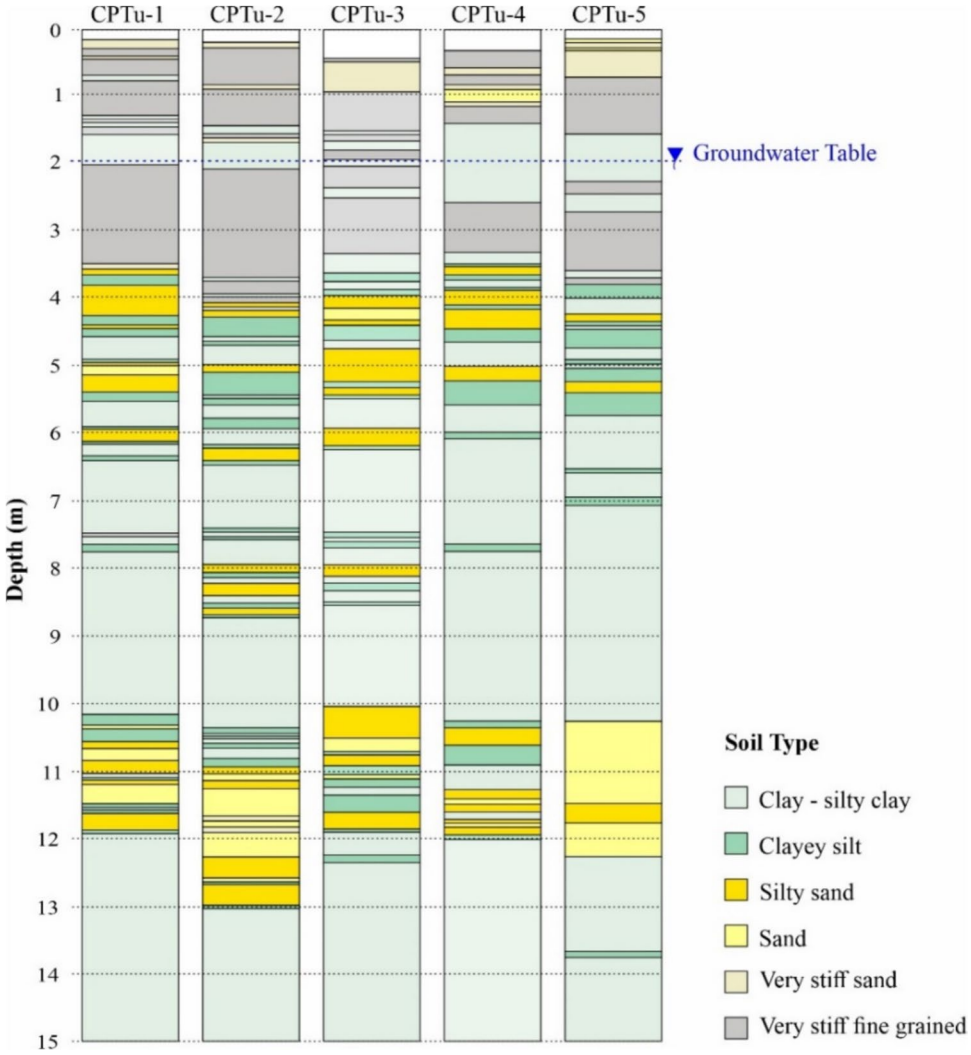


Fig. 7 A generalized subsurface profile of the study area created using CPTu data

Table 6 Shear strength parameters of undisturbed samples

S.S.	c (kPa)	ϕ (°)	S.S.	c (kPa)	ϕ (°)
1	21.2	31	11	8.6	34
2	19.7	28	12	17.9	31
3	46.1	22	13	17.9	30
4	41.9	27	14	36.6	26
5	6.6	32	15	4.1	33
6	23.4	29	16	15.3	32
7	28.9	30	17	28.2	28
8	12.5	31	18	16.7	29
9	6.4	33	19	5.7	32
10	7.9	35	20	21.8	29

Table 7 Shear strength parameters of the resedimented samples

S.S.	$c_{(res)}$ (kPa)	$\phi_{(res)}$ (°)	S.S.	$c_{(res)}$ (kPa)	$\phi_{(res)}$ (°)
1	5.3	30	11	11.7	30
2	11.0	29	12	16.1	29
3	24.5	28	13	18.1	30
4	14.9	29	14	17.4	30
5	15.5	28	15	8.9	31
6	21.6	29	16	16.7	29
7	9.9	31	17	20.9	30
8	18.6	30	18	14.6	30
9	10.6	31	19	6.0	32
10	13.1	30	20	12.2	32

most soil classification systems; therefore, they act as de facto boundary conditions for the models proposed in this study.

Prediction of cohesion

As a result of the MVR analyses, an estimation model was proposed for the cohesion parameter. Table 9 shows model parameters, their significance at 95% CI, and coefficients for

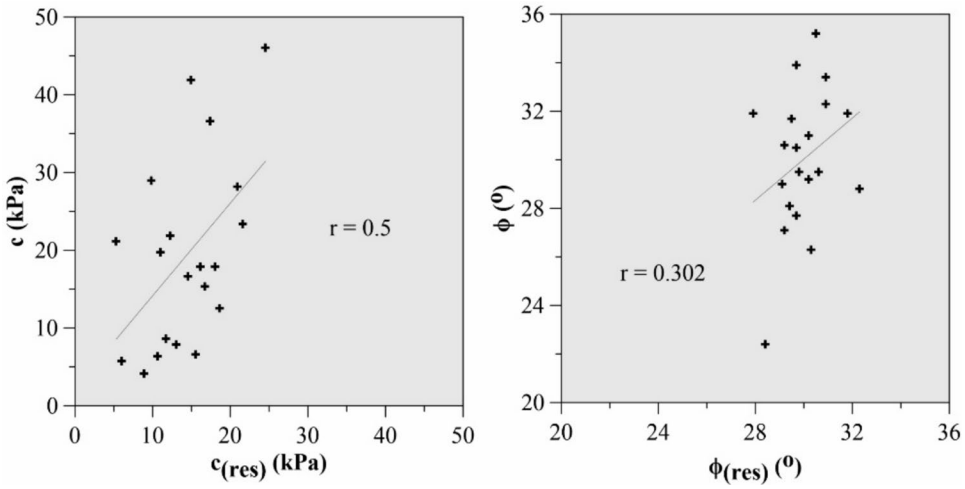


Fig. 8 Scatter plots of the correlation analyses for c and ϕ

Table 8 Dependent and independent variables used in the MVR analyses

Test parameter	Variable type
Cohesion of undisturbed sample, c	Dependent variable
Friction angle of undisturbed sample, ϕ	Dependent variable
Cohesion of resedimented sample, $c_{(res)}$	Independent variable
Friction angle of resedimented sample, ϕ_{res}	Independent variable
Liquid limit of undisturbed sample, LL	Independent variable
Plastic limit of undisturbed sample, PL	Independent variable
Specific gravity of undisturbed sample, G_s	Independent variable
Natural water content of undisturbed sample, ω_n	Independent variable
Void ratio of undisturbed sample, *e*	Independent variable
Saturation degree of undisturbed sample, S_r	Independent variable
Clay percent of undisturbed sample, CP	Independent variable
Silt percent of undisturbed sample, SP	Independent variable

the models. R and R^2 values of the models are also given in Table 9. As can be seen, the model and the predictors included in the model are statistically significant at 95% CI. The predictors used by the model appear to be in line with similar studies in literature. The equation for predicting cohesion is given in Eq. 1. Table 10 shows the cohesion values of the undisturbed samples, and the predicted values determined by the proposed equation. Figure 9 illustrates the results in a scatter plot.

$$c_{(reg)} = 319.28 + 1.36\, c_{(res)} - 71.683e - 1.721\ PL - 84.124\ G_S \quad (1)$$

Prediction of internal friction angle

Two different estimation models were proposed for ϕ. The coefficients for the MVR analyses, along with lower and upper bounds for 95% CI, significance values for the models and each predictor, are shown in Table 11. Model-1 uses the SP predictor in addition to the predictors used in Model-2, with an R^2 value of 0.797 (Eq. 2). But in Model-1 the constant seems statistically insignificant (sig. = 0.404). For most applications of MVR this poses no risk, and the constant can be discarded, but this is not the case for an estimation model since it can affect the results dramatically. Nevertheless, the model itself is statistically significant (sig. = 0.001) as seen in Table 11 and can be used in estimating ϕ. Model-2 uses $c_{(res)}$, PL, and *e* as predictors, and a constant value, all of

Table 9 Result of the MVR analysis for cohesion

	UC*		SC**	Sig	95% CI		R	R^2	Sig
	B	Std. Error	Beta		Lower B	Upper B			
(Constant)	319.28	85.947		0.002	136.088	502.473	0.882	0.778	
$c_{(res)}$	1.36	0.303	0.572	0.000	0.715	2.005			
e	−71.683	18.110	−0.484	0.001	−110.284	−33.080			0.000
PL	−1.721	0.413	−0.634	0.001	−2.600	−0.841			
G_S	−84.124	30.662	−0.429	0.015	−149.479	−18.769			

*Unstandardized coefficients

**Standardized coefficients

Table 10 c values of the undisturbed soil samples and c values estimated by Eq. 1

S.S.	c (kPa)	$c_{(reg)}$ (kPa)	S.S.	c (kPa)	$c_{(reg)}$ (kPa)
1	21.2	10.2	11	8.6	2.0
2	19.7	22.5	12	17.9	25.2
3	46.1	37.5	13	17.9	13.1
4	41.9	32.9	14	36.6	33.8
5	6.6	7.9	15	4.1	6.3
6	23.4	28.2	16	15.3	23.9
7	28.9	27.2	17	28.2	26.5
8	12.5	11.8	18	16.7	24.0
9	6.4	7.8	19	5.7	8.3
10	7.9	10.9	20	21.8	27.0

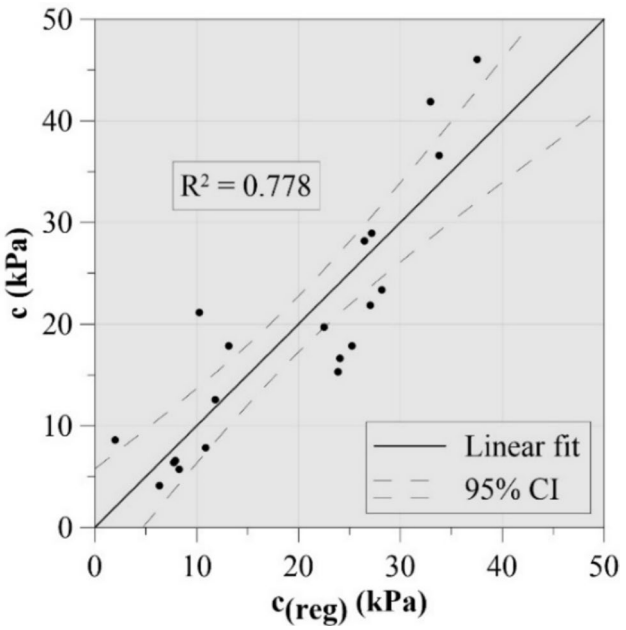


Fig. 9 Scatter plot of c and $c_{(reg)}$ parameters calculated by Eq. 1

which are statistically significant at 95% CI. The model is also significant, with an R^2 value of 0.723 (Eq. 3). The ϕ values of the undisturbed samples and the $\phi_{(reg)}$ values calculated using Eqs. 2 and 3 are given in Table 12. This data is plotted in Fig. 10.

$$\phi_{(reg1)} = 5.418 - 0.371\, c_{(res)} + 0.493\, PL + 0.117\, SP + 13.756e \quad (2)$$

$$\phi_{(reg2)} = 16.903 - 0.318\, c_{(res)} + 0.337\, PL + 11.171e \quad (3)$$

Model validation

The proposed estimation models were validated in two steps. First, the 4 assumptions of the linear MVR analyses were tested, since all proposed models were linear. In this context, linearity, normality of residuals, homoscedasticity, and absence of multicollinearity were examined using normal probability plots (P-P), residual—predicted plots, and variance inflation factors (VIF). In a second step, the proposed models were replicated using another estimation method, artificial neural networks (ANN). Testing the model using data from similar studies in literature would certainly be the better approach, but there are many significant differences between this study and those in the literature such as the type of the soil used, the stress history of the soil, the methodology of the laboratory compaction process, the laboratory tests conducted, etc. A large number of physical and plastic soil properties were determined in this study, some of which are rarely used in other studies, such as specific gravity and void ratio, which are used as predictors in the estimation models proposed in this study. In addition, there are only a handful of studies where both resedimented and intact shear parameters of the same soil are determined or evaluated (e.g., Burland 1990; House 2012; Casey et al.

Table 11 Result of the MVR analysis for internal friction angle

Model		UC*		SC**	Sig	95% CI		R	R^2	Sig
		B	Std. Err	Beta		Lower B	Upper B			
1	(Constant)	5.418	6.311		0.404	−8.034	18.871	0.893	0.797	0.001
	$c_{(res)}$	−0.371	0.071	−0.645	0.001	−0.522	−0.220			
	PL	0.493	0.102	0.751	0.001	0.276	0.710			
	SP	0.117	0.050	0.386	0.034	0.010	0.224			
	e	13.756	4.338	0.384	0.006	4.509	23.003			
2	(Constant)	16.903	4.474		0.002	7.417	26.388	0.850	0.723	0.000
	$c_{(res)}$	−0.318	0.76	−0.553	0.001	−0.479	−0.158			
	PL	0.337	0.87	0.513	0.001	0.153	0.521			
	e	11.171	4.743	0.312	0.032	1.116	21.226			

*Unstandardized coefficients

**Standardized coefficients

Table 12 ϕ values of the undisturbed soil samples and $\phi_{(reg)}$ values estimated by Eqs. 2 and 3

S.S.	ϕ (°)	$\phi_{(reg1)}$ (°)	$\phi_{(reg2)}$ (°)	S.S.	ϕ (°)	$\phi_{(reg1)}$ (°)	$\phi_{(reg2)}$ (°)
1	31.0	32.7	30.8	11	33.9	34.8	32.4
2	28.1	28.6	28.0	12	30.6	28.7	27.4
3	22.4	24.0	23.2	13	29.5	30.1	28.2
4	27.1	27.6	28.7	14	26.3	26.1	27.1
5	31.9	31.2	27.9	15	33.4	33.4	31.4
6	29.0	27.3	26.7	16	31.7	30.1	27.8
7	29.5	29.1	29.7	17	27.7	30.3	28.6
8	30.5	30.6	29.2	18	29.2	30.2	28.8
9	32.3	31.8	33.0	19	31.9	32.4	30.8
10	35.2	32.5	31.1	20	28.8	28.4	28.3

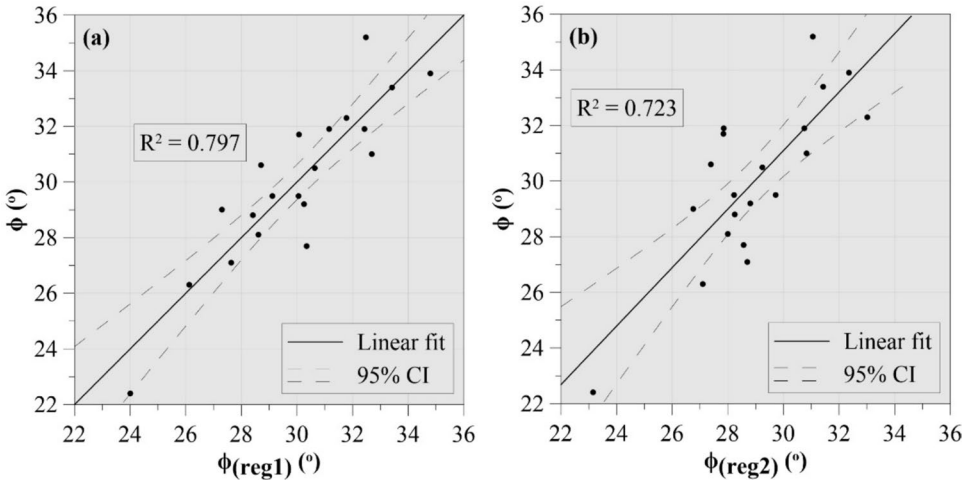


Fig. 10 Scatter plots of ϕ and $\phi_{(reg)}$ parameters calculated by Eq. 2 (**a**) and Eq. 3 (**b**)

2015b), while the estimation models proposed in this study rely entirely on these parameters. Therefore, the validation approach explained above was adopted in this study.

Testing the assumptions of linear regression

Normality of residuals

The vertical distance between a data point and the regression line is called a residual. In a valid linear regression analysis, the residuals are expected to be normally distributed. Therefore, normality of residuals was tested using normal P-P for all estimation models proposed in the study. Ideally, the data points in normal P-P should follow the normality line, which is the case for all the models as seen in Fig. 11, which indicates the residuals in the models are normally distributed.

Homoscedasticity

Homoscedasticity indicates that the residuals are evenly distributed across the range of predicted values. It can be checked using residual-predicted plots. The data points in the plots should resemble a "shotgun blast", i.e. no observable pattern or accumulation. In Fig. 12, it can be seen that the data points are scattered across the plot area and there is no sign of any particular pattern.

Linearity

Linearity indicates a linear relationship between dependent and independent variables used in the analysis. This assumption was assessed using a matrix plot depicting scatterplots of all variables used in the MVR analysis (Fig. 13). As can be seen, no non-linear relationship was observed between the variables.

Absence of multicollinearity

Multicollinearity occurs when independent variables are highly correlated with each other, which obscures the results of the MVR analysis and can lead to incorrect inferences. VIFs are used in this study to check for multicollinearity in the data (Table 13). VIF values above 10 indicate serious multicollinearity, whereas values below 5 are ideal. As seen in Table 13, all VIF values are below 5, indicating independent variables are not correlated with each other.

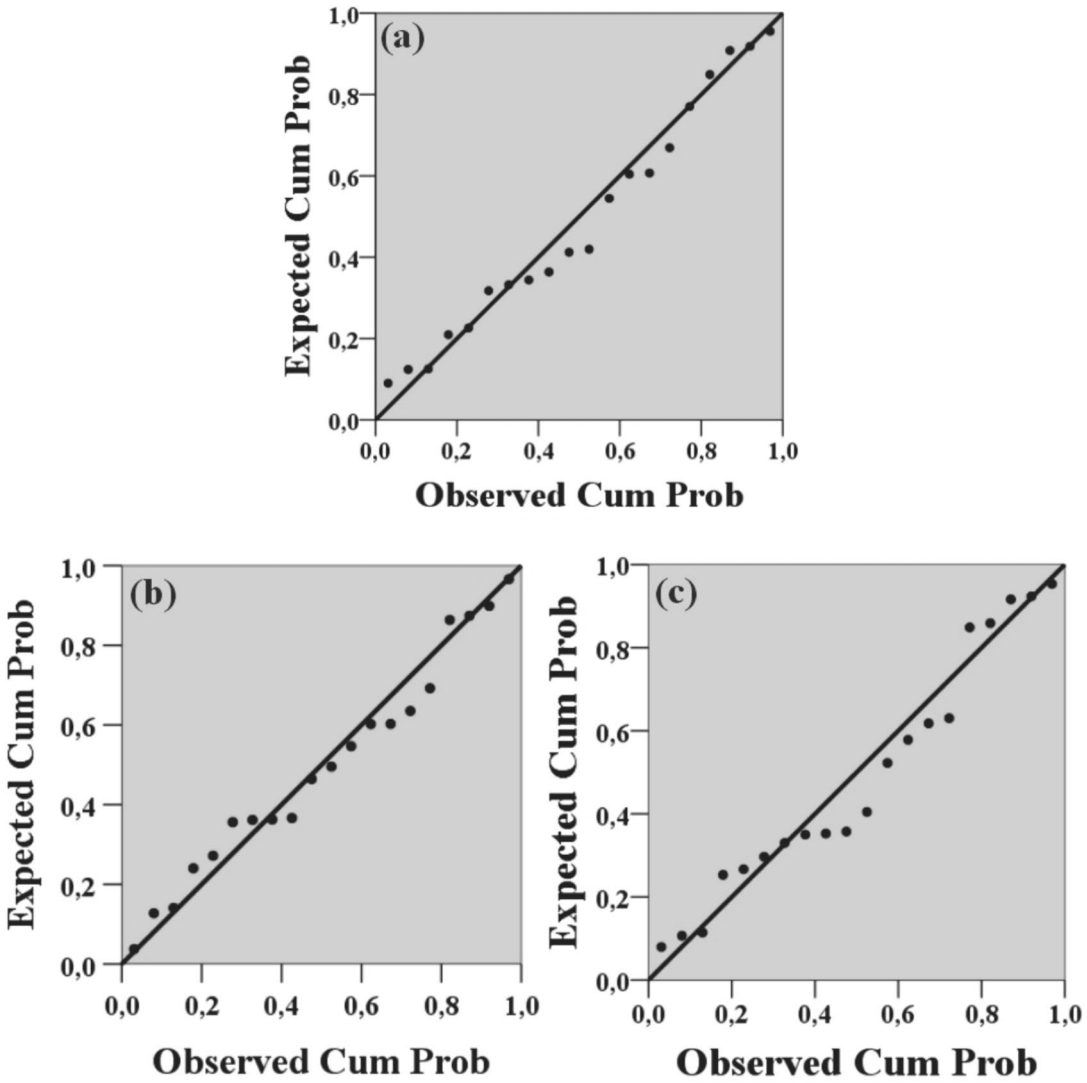


Fig. 11 Normal P-P of the estimation models for $c_{(reg)}$ (**a**), $\phi_{(reg1)}$ (**b**), and $\phi_{(reg2)}$ (**c**)

ANN analyses

ANN is a computer-based method that basically mimics the functioning of the human brain and enables many processes such as associating complex data, making predictions and forecasts based on these data, clustering, filtering, optimizing, etc. The ANN module of the SPSS® v23 software was utilized, and multilayer perceptron, one of the most popular ANN methods, was used in the analyses. This method uses a guided learning technique called back-propagation to train the data and consists of at least 3 layers: input, hidden, and output. The input layer contains the parameters to be used in the ANN analysis as 'nodes' or neurons. The hidden layer contains the stages of training the data and retraining the errors with feedback. The output layer contains the data obtained as a result of the analysis.

In the ANN analyses, the same predictors as in the MVR were used for each estimation model. Our objective was to reproduce the predicted values of $c_{(reg)}$, $\phi_{(reg1)}$ and $\phi_{(reg2)}$ using ANN, while obtaining R^2 values as close as possible to the MVR analyses. Figures 14 and 15 illustrate the results of ANN analyses conducted for $c_{(reg)}$, $\phi_{(reg1)}$ and $\phi_{(reg2)}$, respectively. Fairly similar results to the MVR analyses were obtained, especially for cohesion, where $c_{(reg)}$ values are almost identical to $c_{(ann)}$ values (Fig. 14b). The R^2 values of the models developed by ANN and MVR are also quite close (Fig. 14a), which indicates both methods developed very similar models to estimate cohesion. The same comments can be made for $\phi_{(reg1)}$ and $\phi_{(reg2)}$. Even though the results indicate ANN and MVR developed slightly different models to predict ϕ (Fig. 15a, c), the predicted values are comparable, especially for $\phi_{(reg1)}$ (Fig. 15b, d).

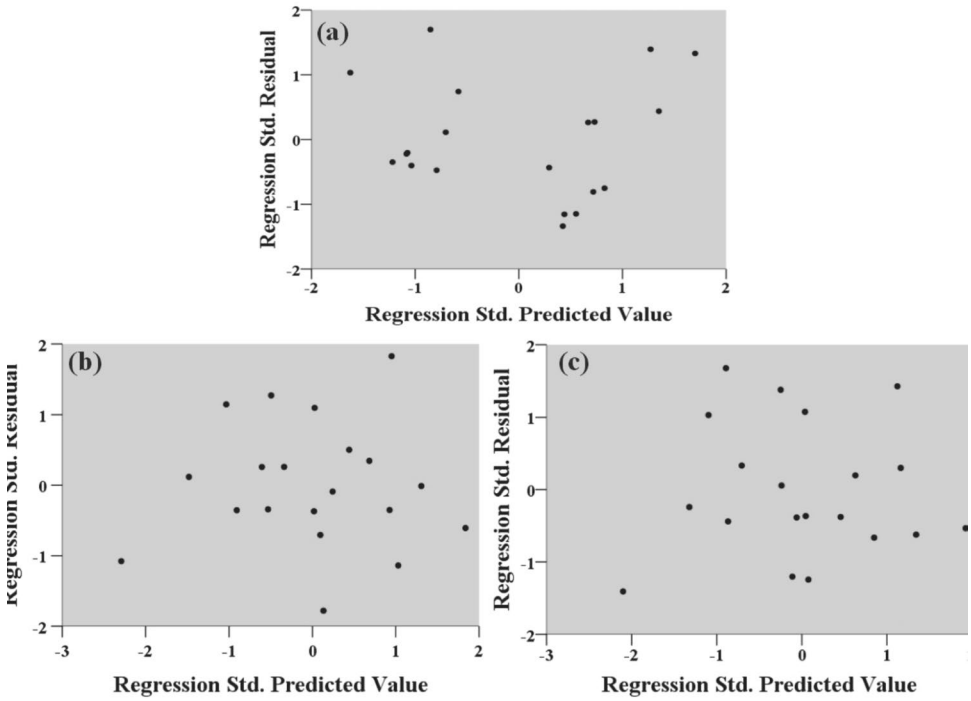


Fig. 12 Residual-predicted charts of the estimation models for $c_{(reg)}$ (**a**), $\phi_{(reg1)}$ (**b**), and $\phi_{(reg2)}$ (**c**)

Discussion

Unlike marine sediments, which are deposited in a relatively stable and homogeneous environment, alluvial soils are formed either in riverbeds or river deltas, which are quite volatile and heterogeneous in terms of depth, characteristics of the suspended material, groundwater levels, and deposition rate, among other aspects of sedimentation. Therefore, substantial differences can be observed between the samples obtained from an alluvial soil profile in terms of grain size, plasticity, saturation degree, and shear strength. This study is a prime example of this phenomenon where a wide range of strength characteristics are observed in laboratory tests with *c* values varying between 4.1 and 46.1 kPa, and ϕ values varying between 26 and 35º. *c* values seem consistent with the physical and index properties of the samples and literature data. However, it is evident that the ϕ values of both undisturbed and resedimented samples determined in this study are above expectations. The reasons for the high ϕ values for undisturbed samples are that (1) the samples are not fully saturated ($90.4\% \leq S_r \leq 97.5\%$), (2) the plasticity of the samples is generally low, and (3) the soils are lightly to moderately over-consolidated ($2 \leq OCR \leq 9$). In UU triaxial tests conducted on samples that are not fully saturated, a certain degree of consolidation occurs within the sample even though drainage is not allowed, which results in a curved Mohr's failure envelope (ASTM 2015). Consequently, internal friction angle values exceeding zero are obtained. If implementation of fully UU conditions is necessary, the samples should be saturated prior to testing using an appropriate saturation method (such as vacuum saturation or back pressure saturation). In addition, even though the samples used in this are not fully saturated, the possible effects of matric suction on the shear strength parameters are neglected since the undisturbed samples are obtained below the GWT, where it is known that matric suction is equal to zero (Fredlund 2006). However, as the samples used in the triaxial tests were not fully saturated, the test results could be affected by matric suction, which may also explain the high internal friction angle values obtained (Wu et al. 2022; Abd et al. 2020; Ibrahim 2015). There are also some studies that report peak or effective internal friction angle values up to 45° for natural clays and over-consolidated fine-grained soils (Diaz-Rodriguez et al. 1992; Ouyang and Mayne 2018; Arvanitidis et al. 2019). Therefore, unusually high ϕ values are sometimes encountered in certain circumstances where OCR, saturation degree, grain size distribution, and drainage conditions play a significant role. It should be noted that since the intact samples are not fully saturated, partial drainage is likely to occur within the sample during UU triaxial tests, resulting in effective stress conditions.

Unsaturated conditions were also observed in UU tests conducted on resedimented samples ($88\% \leq S_r \leq 97\%$), probably due to the matric suction occurring after the sample is taken out of the consolidometer. In addition, as mentioned in Sect. "Resedimentation procedure", resedimented samples were prepared from materials passing through a #100 sieve. Therefore, it is conceivable that the samples vary in their composition, with some being predominantly clay and others primarily silt. This variation in composition could account

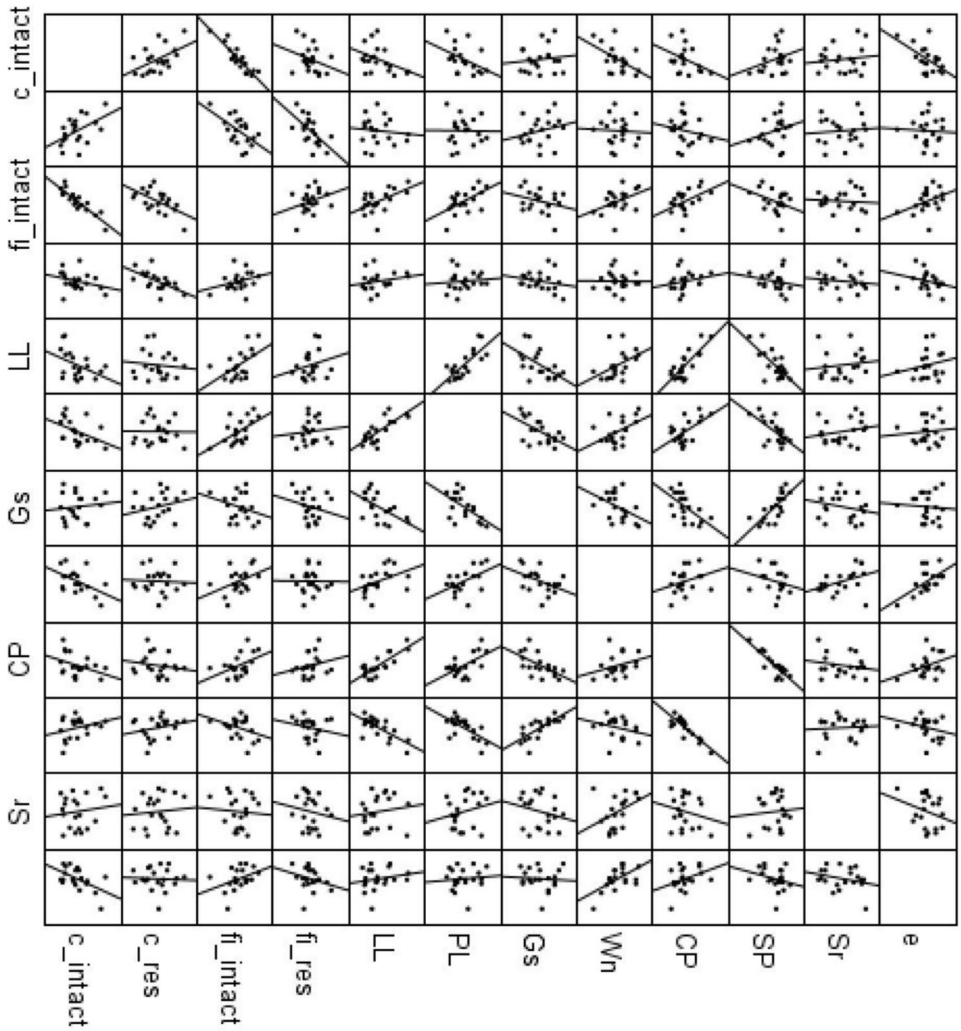


Fig. 13 Matrix plot containing the scatterplots of dependent and independent variables used in MVR analyses

Table 13 Collinearity statistics of the proposed estimation models

Model	Independent variable	Collinearity statistics	
		Tolerance	VIF
$c_{(reg)}$	$c_{(res)}$	0.913	1.095
	e	0.988	1.012
	PL	0.638	1.566
	G_S	0.604	1.657
$\phi_{(reg1)}$	$c_{(res)}$	0.896	1.117
	PL	0.563	1.777
	SP	0.496	2.014
	e	0.924	1.082
$\phi_{(reg2)}$	$c_{(res)}$	0.997	1.003
	PL	0.991	1.009
	e	0.988	1.012

for the higher internal friction angle values observed in the resedimented samples. This is a fundamental but inevitable drawback, as it would be practically impossible to separate clay and silt particles when preparing the resedimented sample.

It has been noted that the ϕ values of the resedimented and undisturbed samples are comparable in terms of the scatter of the data, i.e., upper and lower bounds of ϕ and $\phi_{(res)}$ values are close (Fig. 16). Considering that ϕ is closely related to the size of the soil grains and that samples with very similar grain size distributions to the original samples were used in the resedimentation process, it can be said that this situation is to be expected. On the contrary, *c* values of the resedimented samples are generally lower than the those of the undisturbed samples and are distributed much more narrowly. This may be due to the fact that *c* depends on various parameters such as aging and soil structure (Zriek et al. 1998). During resedimentation, despite waiting until the end of secondary compression, the soil structure may not have reached a level close to the original sample. It may be possible to prevent this situation by waiting for more than one logarithmic cycle of secondary compression during resedimentation, or by

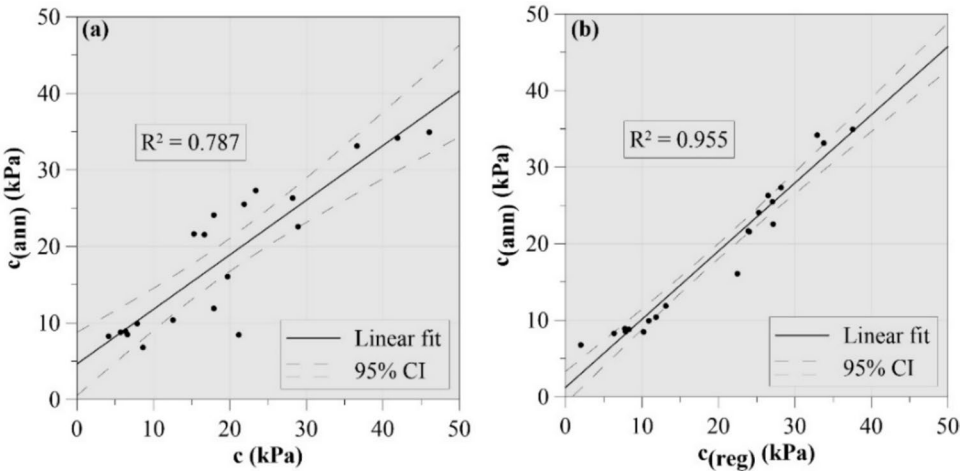


Fig. 14 Scatter plots of ANN-predicted $c_{(ann)}$ versus intact sample c (**a**) and MVR-predicted $c_{(reg)}$ (**b**)

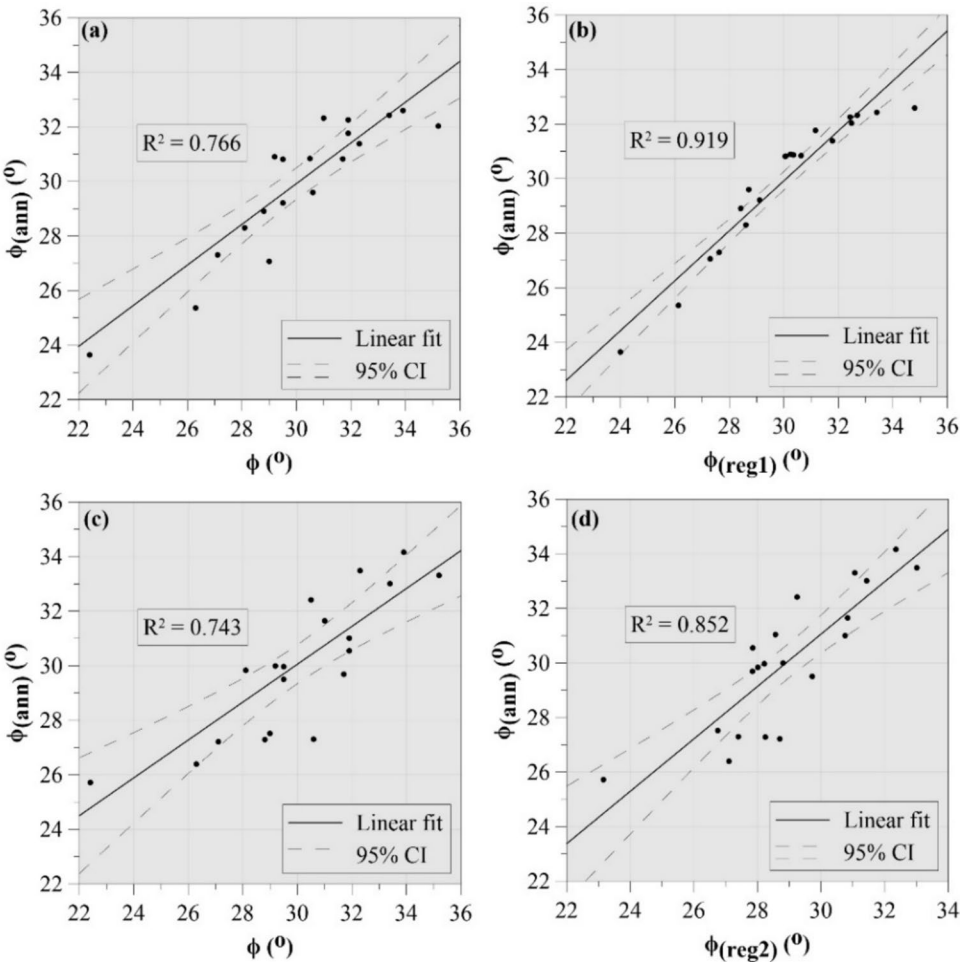


Fig. 15 Scatter plots of ANN-predicted $\phi_{(ann)}$ versus intact sample ϕ (**a**, **c**) and MVR-predicted $\phi_{(reg1)}$ and $\phi_{(reg2)}$ (**b**, **d**)

adding various chemicals to the water used (Germaine and Ladd 1988). In contrast, for undisturbed samples with low cohesion values (approximately ≤ 10 kPa), resedimentation appears to increase cohesion. This is likely due to the modified soil structure during the consolidation phase (Delage and Lefebvre 1984), and the possible differences in grain sizes that could be present in the resedimented samples.

The first phase of the statistical analyses compared the shear strength parameters of undisturbed and resedimented samples to investigate a possible relationship between the

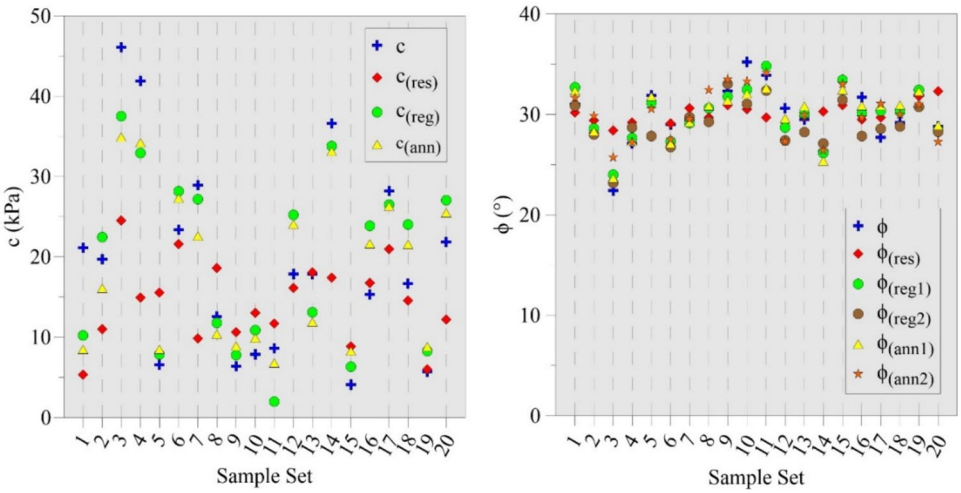


Fig. 16 Scatter plots of all parameters determined and estimated within the scope of the study

Table 14 The estimation models for c and ϕ developed by MVR analyses

Equation	R	R^2
$c_{(reg)} = 319.28 + 1.36\ c_{(res)} - 71.683\ e - 1.721\ PL - 84.124\ G_S$	0.882	0.778
$\phi_{(reg1)} = 5.418 — 0.371\ c_{(res)} + 0.493\ PL + 0.117\ SP + 13.756\ e$	0.893	0.797
$\phi_{(reg2)} = 16.903 — 0.318\ c_{(res)} + 0.337\ PL + 11.171\ e$	0.850	0.723

parameters. The correlation analyses yielded R values of 0.5 and 0.302, respectively, between $c - c_{(res)}$ and $\phi - \phi_{(res)}$. This indicates a very poor relationship between the intact and resedimented shear strength parameters of the samples. This is contrary to the studies in the literature where similar shear strength and shear behavior are observed between the intact and laboratory-compacted specimens of fine-grained marine sediments (Burland 1990, Casey et al. 2015b, and House 2012). It seems that the resedimentation method is best representative of marine environments where the depositional factors such as water velocity, bed depth, characteristics of the incoming material, etc. do not change drastically in both spatial and temporal dimensions, unlike alluvial depositional environments.

MVR analyses were performed on a larger number of variables to establish a more reliable predictive model. In addition to the shear strength parameters, this analysis also included the liquid limit (LL), plastic limit (PL), unit volume weight (γ), specific gravity (G_s), void ratio (*e*), clay percent (CP), silt percent (SP), water content (ω), and degree of saturation (S_r) of the soil samples. The results of the MVR analysis are summarized in Table 14.

There is an extensive amount of variety in the predictors used in the estimation models in literature, such as LL, PL, PI, and I_C, among many others (Sharma and Bora 2003; Mousavi et al. 2011; Sørensen and Okkels 2013; Stark and Hussain 2013). Hence, the predictors used in the estimation models proposed in this study appear to be in line with the previous studies. An interesting point is that $c_{(res)}$ is used as a predictor in both models to estimate ϕ, instead of $\phi_{(res)}$. This is indicative of a stronger negative relationship between $\phi_{(reg)}$ and $c_{(res)}$ than a positive relationship between $\phi_{(reg)}$ and $\phi_{(res)}$, which is understandable considering the higher degree of correlation between c and $c_{(res)}$.

The proposed estimation models are statistically significant for $p \leq 0.05$ and have high enough R^2 values to be considered as accurate. Yet, it should be noted that a set of 20 samples were used in this study, which is generally considered as the minimum number of samples for a healthy MVR analysis. A larger sample size would certainly be of benefit to the wider application of the proposed models. Also, the boundary conditions for the models should be carefully considered because they are substantially different from the ones described in literature due to the origin and characteristics of the soils used in this study. Unfortunately, the differences in boundary conditions also prevented validating the models proposed in this study using the literature data. The estimation models were validated by checking the assumptions of linear regression, performing case-wise significance and variance analyses, and comparing the predicted values with the ones obtained from ANN analyses. Figure 16 depicts the c and ϕ values of the undisturbed samples determined in this study, as well as the values predicted by MVR and ANN analyses.

Conclusions

This study proposes empirical equations for predicting shear strength parameters, c and ϕ, of fine-grained alluvial soils using resedimented samples. Undisturbed alluvial soil samples were collected from the field, and their index

and physical properties were determined, along with shear strength parameters. The samples were then resedimented in the laboratory to replicate their original field conditions, and their shear strength parameters were determined. Finally, multivariate regression analyses were conducted using all the determined parameters to predict the shear strength parameters of the undisturbed samples. Estimation models that are statistically significant at 95% confidence interval, and have R^2 values above 0.7 were developed for c and ϕ. These main conclusions that can be derived from the study:

(1) The resedimentation method is best suited for samples formed in a marine environment where depositional factors such as deposition rate, water velocity, bed depth, and characteristics of the material being deposited are relatively constant both spatially and temporarily, unlike alluvial depositional environments such as riverbeds and river deltas.
(2) The ϕ values of the undisturbed and resedimented samples have similar upper and lower bounds, but they are poorly correlated.
(3) The c values of the resedimented samples are generally lower than the undisturbed samples. Although the resedimented samples are loaded for a log cycle of secondary compression during resedimentation, it is probably not enough for the soil sample to regain its in-situ texture, structure, and/or bonding.
(4) Shear strength parameters of the resedimented samples alone are not sufficient to estimate the shear strength parameters of the undisturbed samples, at least for the alluvial soils used in this study. Other soil parameters such as physical and index properties should also be included in the statistical analyses.
(5) c and ϕ values of the undisturbed samples can be predicted with an acceptable accuracy using the estimation models developed by MVR analyses. The models use easily available soil parameters, along with shear strength parameters of the resedimented samples. This approach can be useful in certain circumstances where undisturbed soil samples cannot be obtained from the field due to economic, logistical, or other reasons.
(6) Validation of the models using literature data was not possible due to substantial differences in boundary conditions. Also, sample sizes for the statistical analyses are relatively low. Further studies on the shear strength of resedimented alluvial soils are needed to enhance the applicability of the proposed estimation models.

Acknowledgements The authors would like to express their gratitude to Mr. Emrah Ocak, who provided invaluable assistance in drilling studies. They would also like to acknowledge the contributions of Mr. Ozan Şahin and Mr. İlkay Çay, who played a significant role in the production of the consolidometer test device. This study would not have been possible without the invaluable contributions of Dr. Arzu Fırat Ersoy and Dr. İrfan Temizel, who provided support during the determination of borehole locations. Additionally, Dr. Brendan Casey provided invaluable insights into the resedimentation method.

Author contributions MOS: Conceptualization, methodology, investigation, formal analysis, writing—original draft. HE: Conceptualization, supervision, funding acquisition, writing – review & editing.

Funding Open access funding provided by the Scientific and Technological Research Council of Türkiye (TÜBİTAK). This study was supported by the Scientific Research Projects Coordination Unit of Karadeniz Technical University (project numbers FBA-2019–8434 and FDK-2019–8228).

Data availability No datasets were generated or analysed during the current study.

Declarations

Conflict of interest The authors declare that they have no known competing financial interests or personal relationships that could have appeared to influence the work reported in this paper.

Open Access This article is licensed under a Creative Commons Attribution 4.0 International License, which permits use, sharing, adaptation, distribution and reproduction in any medium or format, as long as you give appropriate credit to the original author(s) and the source, provide a link to the Creative Commons licence, and indicate if changes were made. The images or other third party material in this article are included in the article's Creative Commons licence, unless indicated otherwise in a credit line to the material. If material is not included in the article's Creative Commons licence and your intended use is not permitted by statutory regulation or exceeds the permitted use, you will need to obtain permission directly from the copyright holder. To view a copy of this licence, visit http://creativecommons.org/licenses/by/4.0/.

References

Abd IA, Fattah MY, Mekkiyah H (2020) Relationship between the matric suction and the shear strength in unsaturated soil. Case Stud Constr Mater 13:e00441. https://doi.org/10.1016/j.cscm.2020.e00441

Abdulhadi NO, Germaine JT, Whittle AJ (2012) Stress-dependent behavior of saturated clay. Can Geotech J 49:907–916. https://doi.org/10.1139/t2012-057

Abdulhadi NO (2009) An experimental investigation into the stress-dependent mechanical behavior of cohesive soil with application to wellbore instability. Dissertation, Massachusetts Institute of Technology.

Adams AL, Nordquist TJ, Germaine JT, Flemings PB (2016) Permeability anisotropy and resistivity anisotropy of mechanically compressed mudrocks. Can Geotech J 53:1474–1482. https://doi.org/10.1139/cgj-2015-0596

Arvanitidis C, Steiakakis E, Agioutantis Z (2019) Peak friction angle of soils as a function of grain size. Geotech Geol Eng 37:1155–1167. https://doi.org/10.1007/s10706-018-0675-8

ASTM (2015) Standard Test Method for Unconsolidated-Undrained Triaxial Compression Test on Cohesive Soils. ASTM D2850–15, ASTM International, West Conshohocken.

Aydın M, Demir O, Serdar HS, Özaydın S, Harput B (1995) Tectono-sedimentary evolution and hydrocarbon potential of the Sinop-Boyabat Basin, North Turkey. In: Erler A (ed) Geology of the

Black Sea Region. General Directorate of Mineral Research and Exploration, Ankara. pp 254–263
Burland JB (1990) On the compressibility and shear strength of natural clays. Géotechnique 40:329–378. https://doi.org/10.1680/geot.1990.40.3.329
Casey B, Germaine JT, Flemings PB, Fahy BP (2015a) Estimating horizontal stresses for mudrocks under one-dimensional compression. Mar Pet Geol 65:178–186. https://doi.org/10.1016/j.marpetgeo.2015.02.001
Casey B, Reece JS, Germaine JT (2019) One-dimensional normal compression laws for resedimented mudrocks. Mar Pet Geol 103:397–403. https://doi.org/10.1016/j.marpetgeo.2019.02.023
Casey B, Germaine JT, Reynolds RT (2015b) The strength behavior of resedimented Presumpscot clay and a comparison with intact behavior. In: London ME, Nickerson C (ed) Proc., 2nd Symp. on the Presumpscot Formation: Advances in Geotechnical, Geologic, and Construction Practice. University of Maine, Portland
Cunningham MR, Ridley AM, Dineen K, Burland JB (2003) The mechanical behaviour of a reconstituted unsaturated silty clay. Géotechnique 53:183–194. https://doi.org/10.1680/geot.2003.53.2.183
Delage P, Lefebvre G (1984) Study of the structure of a sensitive Champlain clay and of its evolution during consolidation. Can Geotech J 21:21–35. https://doi.org/10.1139/t84-003
Diaz-Rodriguez JA, Leroueil S, Aleman JD (1992) Yielding of Mexico City clay and other natural clays. J Geotech Eng 118:981–995. https://doi.org/10.1061/(ASCE)0733-9410(1992)118:7(981)
Ersoy H, Karsli MB, Cellek S, Kul B, Baykan I, Parsons RL (2013) Estimation of the soil strength parameters in Tertiary volcanic regolith (NE Turkey) using analytical hierarchy process. J Earth Syst Sci 122:1545–1555. https://doi.org/10.1007/s12040-013-0366-z
Eyuboglu Y, Chung SL, Santosh M, Dudas FO, Akaryalı E (2011) Transition from shoshonitic to adakitic magmatism in the Eastern Pontides, NE Turkey: implications for slab window melting. Gondwana Res 19:413–429. https://doi.org/10.1016/j.gr.2010.07.006
Fredlund DG (2006) Unsaturated soil mechanics in engineering practice. J Geotech Geoenviron Eng 132:286–321. https://doi.org/10.1061/(ASCE)1090-0241(2006)132:3(286)
Gedik A, Korkmaz S (1984) Geology of the Sinop basin and petroleum possibilities. J Geol Eng 19:53–80
Gedik A, Ercan T, Korkmaz S (1984) The geology of the Middle Black Sea (Samsun-Sinop) basin and the petrology of the volcanic rocks. Bul Min Res Exp 99:34–50
Germaine JT, Ladd CC (1988) Triaxial testing of saturated cohesive soils. In: Advanced triaxial testing of soil and rock. pp 421–459. https://doi.org/10.1520/STP29091S
Goktepe AB, Altun S, Altintas G, Tan O (2008) Shear strength estimation of plastic clays with statistical and neural approaches. Build Environ 43:849–860. https://doi.org/10.1016/j.buildenv.2007.01.022
Gorur N, Tuysuz O (2001) Cretaceous to Miocene palaeogeographic evolution of Turkey: implications for hydrocarbon potential. J Pet Geol 24:119–146. https://doi.org/10.1111/j.1747-5457.2001.tb00664.x
House RD (2012) A comparison of the behavior of intact and resedimented Boston Blue Clay (BBC). Dissertation, Massachusetts Institute of Technology
Huang Y, Swan C (2017) Evaluating the behavior of a cohesive soil undergoing one cycle of freeze-thaw. Proc Geotechnical Frontiers 2017:643–651
Ibrahim KMHI (2015) Effect of percentage of low plastic fines on the unsaturated shear strength of compacted gravel soil. Ain Shams Eng J 6:413–419. https://doi.org/10.1016/j.asej.2014.10.012
Kayabali K, Tufenkci OO (2010) Shear strength of remolded soils at consistency limits. Can Geotech J 47:259–266. https://doi.org/10.1139/T09-095
Khaboushan EA, Emami H, Mosaddeghi MR, Astaraei AR (2018) Estimation of unsaturated shear strength parameters using easily-available soil properties. Soil Tillage Res 184:118–127. https://doi.org/10.1016/j.still.2018.07.006
Kul Yahşi B, Ersoy H (2021) Effect of mineralogical composition related to profile depth on index and strength properties of regolith soil. B Eng Geol Environ 80:1791–1808. https://doi.org/10.1007/s10064-020-01968-8
Ladd CC, Varallyay J (1965) The influence of stress system on the behavior of saturated clays during undrained shear. Massachusetts Institute of Technology, pp 266
Locat J, Lefebvre G (1985) The compressibility and sensitivity of an artificially sedimented clay soil: The Grande-Baleine Marine Clay, Québec, Canada. Mar Georesour Geotec 6:1–28. https://doi.org/10.1080/10641198509388178
Marjanovic J (2016) Stiffness characterization of mechanically-compressed cohesive soils using wave propagation. Dissertation, Massachusetts Institute of Technology.
Miao L, Jing F, Houston SL (2006) Soil-water characteristic curve of remolded expansive soils. In: Unsaturated Soils. pp 997–1004. https://doi.org/10.1061/40802(189)8
Mohammadi M, Fatemi Aghda SM, Talkhablou M, Cheshomi A (2022) Prediction of the shear strength parameters from easily-available soil properties by means of multivariate regression and artificial neural network methods. Geomech Geoengin 17:442–454. https://doi.org/10.1080/17486025.2020.1778194
Mousavi SM, Alavi AH, Gandomi AH, Mollahasani A (2011) Nonlinear genetic-based simulation of soil shear strength parameters. J Earth Syst Sci 120:1001–1022. https://doi.org/10.1007/s12040-011-0119-9
Nordquist TJ (2015) Permeability anisotropy of resedimented mudrocks. Dissertation, Massachusetts Institute of Technology.
Okay AI (2008) Geology of Turkey: a synopsis. Anschnitt 21:19–42
Ouyang Z, Mayne PW (2018) Effective friction angle of clays and silts from piezocone penetration tests. Can Geotech J 55:1230–1247
Pham BT, Amiri M, Nguyen MD, Ngo TQ, Nguyen KT, Tran HT et al (2021) Estimation of shear strength parameters of soil using optimized inference intelligence system. Vietnam J Earth Sci. 43:189–198. https://doi.org/10.15625/2615-9783/15926
Rabbani A, Samui P, Kumari S (2023) Optimized ANN-based approach for estimation of shear strength of soil. Asian J Civ Eng 24:3627–3640. https://doi.org/10.1007/s42107-023-00739-6
Ranjpour D (2020) Stiffness and Anisotropy Characterization of Mechanically-Compressed Cohesive Soils Using Directional Wave Propagation. Dissertation, Tufts University.
Robertson PK (1990) Soil classification using the cone penetration test. Can Geotech J 27:151–158. https://doi.org/10.1139/t90-014
Robertson PK (2009) Interpretation of cone penetration tests—a unified approach. Can Geotech J 46:1337–1355. https://doi.org/10.1139/T09-065
Santagata M, Kang YI (2007) Effects of geologic time on the initial stiffness of clays. Eng Geol 89:98–111. https://doi.org/10.1016/j.enggeo.2006.09.018
Seah TH (1990) Anisotropy of resedimented Boston blue clay. Dissertation, Massachusetts Institute of Technology.
Sørensen KK, Okkels N (2013) Correlation between drained shear strength and plasticity index of undisturbedoverconsolidated clays. In: Proceedings of the 18th international conference on soil mechanics and geotechnicalengineering: challenges and innovations in geotechnics/Défis et innovations en géotechnique, vol 1. Presses des Ponts, pp. 423–428
Stark TD, Hussain M (2013) Empirical correlations: drained shear strength for slope stability analyses. J GeotechnGeoenviron Eng

139:853–862. https://doi.org/10.1061/(ASCE)GT.1943-5606.0000824

Sünnetci MO, Ersoy H (2021) Investigating liquefaction potential of alluvial soils in Sahilkent (Bafra, Samsun) area using CPT data. Gümüşhane Univ J Sci Tech Inst. 11:288–304. https://doi.org/10.17714/gumusfenbil.811876

Sünnetci MO (2022) Determination of undrained shear strength parameters of undistrubed samples using the data obtained by resedimentation method. Dissertation, Karadeniz Technical University.

Temizel I, Arslan M, Yücel C, Abdioğlu E, Ruffet G (2016) Geochronology and geochemistry of Eocene-aged volcanic rocks around the Bafra (Samsun, N Turkey) area: Constraints for the interaction of lithospheric mantle and crustal melts. Lithos 258:92–114. https://doi.org/10.1016/j.lithos.2016.04.023

Tran QA, Ho LS, Le HV, Prakash I, Pham BT (2022) Estimation of the undrained shear strength of sensitive clays using optimized inference intelligence system. Neural Comput Appl 34:7835–7849. https://doi.org/10.1007/s00521-022-06891-5

Turoğlu H (2010) Geomorphological features of Kizilirmak delta and its close vicinity, and effects on human life. Anatolian Res 19:99–111

Wang Q, Xu Y, Su W, Ye W, Chen Y, Lai H (2023) Enhancement mechanism of remolding on the swelling behavior of expansive stiff clay: from microstructure perspective. Environ Earth Sci 82:378. https://doi.org/10.1007/s12665-023-11071-2

Wu R, Yang G, Li S, Xiang Q (2022) Experimental study on the effects of matric suction on shear properties of polypropylene fiber reinforced unsaturated clay. Materials 15:8223. https://doi.org/10.3390/ma15228223

Zhu L, Liao Q, Wang Z, Chen J, Chen Z, Bian Q, Zhang Q (2022) Prediction of soil shear strength parameters using combined data and different machine learning models. Appl Sci 12:5100. https://doi.org/10.3390/app12105100

Zreik DA, Germaine JT, Ladd CC (1998) Effect of aging and stress history on the undrained strength of ultra-weak cohesive soils. Soils Found 38(4):31–39

Publisher's Note Springer Nature remains neutral with regard to jurisdictional claims in published maps and institutional affiliations.